Brain, Behavior, and Immunity 137 (2026) 106879

Contents lists available at ScienceDirect

Brain Behavior and Immunity

journal homepage: www.elsevier.com/locate/ybrbi

Full-length Article

Ventral striatal neuroimmune signalling biases the expression of social memory in male mice

M. Rinaudo [a,b,*], S. Autelitano [a], C. D'Amelio [a], I.Nifo Sarrapochiello [a], G. Puliatti [a], G. Boni [a], R. Sollazzo [a], D.D. Li Puma [a,b], F. Paciello [a,b], F. Natale [a,b], V. Protto [c], G. De Chiara [d], R. Piacentini [a,b], S. Fusco [a,b], C. Grassi [a,b]

[a] Department of Neuroscience, Università Cattolica del Sacro Cuore, 00168 Rome, Italy
[b] Fondazione Policlinico Universitario "A. Gemelli" IRCCS, 00168 Rome, Italy
[c] Department of Infectious Diseases, Istituto Superiore di Sanità,00161 Rome, Italy
[d] Institute of Translational Pharmacology, National Research Council (CNR), 00133 Rome, Italy

ARTICLE INFO

Keywords:
Neuroinflammation
HSV-1
LPS
Social memory
Microglia
Dexamethasone

ABSTRACT

Social behaviours are highly sensitive to inflammatory states. However, the precise contribution of neuroinflammation in the ventral striatum to social memory remains unclear. Using a mouse model of recurrent herpes simplex virus-1 (HSV-1) infection and a complementary model of region-restricted inflammation induced by bilateral intra-ventral striatum lipopolysaccharide (LPS) injection, we show that ventral striatal inflammation impacts social memory expression. Both HSV-1-infected and LPS-treated mice failed to discriminate between old and novel conspecifics, with LPS-treated animals showing a slight preference for the known stimulus. In these animals, social memory alterations were associated with microglial activation, inflammatory signalling, and increased GluA2 expression in the ventral striatum and were not dependent on altered social novelty sensitivity. In both models, behavioural alterations were rescued by dexamethasone treatment. Finally, LPS-induced neuroinflammatory markers in the ventral striatum correlated with preference for the familiar social stimulus. Together, these findings identify ventral striatal inflammation as a key modulator of social memory expression.

1. Introduction

Social behaviours encompass a multitude of interactions between same-species individuals, ranging from affiliative to hostile interactions, social approach, social avoidance, or social memory (Li et al., 2025). The whole behavioural repertoire is governed by an extended network of brain areas, comprising the limbic system (e.g., hippocampus, ventral striatum, amygdala, medial prefrontal cortex) and sensory areas (e.g., olfactory structures, Chen and Hong, 2018, Xu et al., 2021). For instance, social memory relies, within the hippocampal formation, on dorsal CA2 (dCA2), which is crucial for encoding and retrieving social identity (Meira et al., 2018), and ventral CA1 (vCA1), which contains ensembles that represent socially relevant information and relay it to downstream motivational structures (Okuyama et al., 2016), such as the nucleus accumbens (NAc) within the ventral striatum (VS) (Muir et al., 2020). Long-range vCA1 to NAc projections are crucial for storing social memory, whereas vCA1 to the medial prefrontal cortex (mPFC) pathways integrate social cues with contextual and internal-state information (Phillips et al., 2019). The mPFC, in turn, modulates the salience and decision-making components of social interactions and provides top-down control over NAc circuits (Okuyama et al., 2016, Hitti and Siegelbaum, 2014, Murugan et al., 2017, Leroy et al., 2023).

Growing evidence indicates that neuroinflammation can profoundly alter the neural circuitry underlying social behaviour and social memory, particularly by affecting hippocampal and mesolimbic structures (Gorina et al., 2022, Jung et al., 2022). Peripheral immune activation can induce central cytokine release (e.g., IL-1β, TNF-α) that disrupts hippocampal plasticity, impairs dCA2- and vCA1-dependent encoding of social information, leading to deficits in social recognition (Smith et al., 2012, Izumi et al., 2021). Microglial activation within the hippocampus has been shown to reduce synaptic efficacy and suppress activity in circuits required for social memory consolidation (Izumi et al., 2021). In parallel, inflammatory signalling within the VS alters dopamine transmission, motivational salience, and modulates social approach/

* Corresponding author at: Department of Neuroscience, Università Cattolica del Sacro Cuore, 00168 Rome, Italy.
E-mail address: marco.rinaudo@unicatt.it (M. Rinaudo).

https://doi.org/10.1016/j.bbi.2026.106879
Received 9 February 2026; Received in revised form 8 June 2026; Accepted 20 June 2026
Available online 21 June 2026

avoidance, positioning the VS as a key convergence point where the immune state modulates social behaviour (Nakajima et al., 2026, Soares-Cunha et al., 2020). Inflammation can also alter mPFC–VS functional connectivity, shifting social decision-making and altering sensitivity to social reward (Felger et al., 2016).

Recent evidence indicates that the relationship between neuroinflammation and VS activity can produce multifaceted social responses in a way that has not been clarified yet (Inagaki et al., 2015). For example, sickness behaviour, which is caused by inflammation/infections, has always been associated with an increase in social avoidance. However, the novelty of the social stimulus can determine whether neuroinflammation will induce avoidance or approach during sickness behaviour, a phenomenon that has been associated with VS activity (Kopec et al., 2019). Furthermore, most studies have focused their attention on short term effects of inflammatory stimuli on social behaviour, such as in sickness behaviour, which may however be confounded also by state-dependent alterations of brain processes, such as the sensation of "feeling sick", body temperature fluctuations or other autonomic responses, as well as by systemic inflammation (Eisenberger et al., 2017, Rogers et al., 2024, Yamamoto et al., 2025), which may influence behavioural responses independently from neuroinflammatory signalling in a specific area. However, whether neuroimmune signalling in the VS can directly modulate social memory is unknown. Indeed, since multiple neuropsychiatric and neurodegenerative disorders, such as Alzheimer's Disease and mood disorders are associated with aberrant neuroinflammatory signalling in different areas of the limbic system (Troubat et al., 2021; Ambi, 2026), defining the role of neuroinflammation in regulating social memory may help identify novel therapeutic targets as well as early predictive cognitive biomarkers indicative of heightened vulnerability to such diseases.

Therefore, the aim of our study was to determine the direct contribution of VS neuroinflammation to social memory. Using two complementary approaches, a broad neuroinflammation model obtained by viral reactivation in the recurrent herpes simplex virus type-1 (HSV-1) infection mouse model, and a more localized inflammatory manipulation obtained through intracerebral bacterial lipopolysaccharide (LPS) injection, we demonstrate that VS inflammation is sufficient to alter social memory, without impacting overall social novelty sensitivity. Finally, anti-inflammatory treatment was able to rescue social memory in both models, thus highlighting the causal contribution of VS-neuroinflammation to social memory.

2. Materials and methods

2.1. Animals and drugs

Wild-type C57BL/6JRj male mice (ranging from 3 to 5 months of age), derived from the Animal Facility of Catholic University, were employed for this study. Mice were housed under standard laboratory conditions with a 12-hour light/dark cycle, with constant humidity (60-75%), controlled room temperature (RT, 20–22 °C) and food and water provided ad libitum. Lipopolysaccharide (L2630- E. Coli O111:B4, Sigma-Aldrich) was dissolved into physiological solution at a concentration of 2 μg/μL and administered as later described (Hunter et al., 2009). Dexamethasone (D4902, Sigma-Aldrich) was dissolved in ethanol, further diluted in water and then administered to animals at a dose of 5 mg/Kg (Son et al., 2022). The respective vehicle condition received saline solution and or water-diluted ethanol.

2.2. Ethics

All experiments and animal procedures were approved by the Catholic University Ethics Committee and were in accordance with the guidelines of the Italian Ministry of Health (Legislative Decree No. 116/1992) and European Union legislations on animal procedures (Directive No. 86/609/EEC), and were approved by the Italian Ministry of Health, procedure number 565/2024-PR.

2.3. Herpes simplex virus 1 model

The mouse model of recurrent HSV-1 infection in the brain was established in male C57BL/6JRj mice as already described (De Chiara et al., 2019, Li Puma et al., 2019, Li Puma et al., 2023). Virus production (HSV-1, strain F) was performed in VERO cells as previously reported (Protto et al 2024). Animals were divided into two groups: the HSV-1-infected group was infected via inoculation of HSV-1with 2 μL of culture medium containing 1×10^6 plaque forming units of the virus (pfu); and the Mock-infected (hereafter referred to as "Mock") group, which was subjected to the same procedure using PBS. Mice were anesthetized with ketamine (65 mg/Kg) and medetomidine (0.65 mg/Kg) and then infected through labial scarification under biosafety level 2 conditions as previously described (De Chiara et al., 2019, Li Puma et al., 2019, Li Puma et al., 2023). Six weeks after the inoculation of the virus, animals to a thermal stress (TS) session, consisting in 15 min at 43 °C obtained in an ad hoc environment, to induce virus reactivation and its spreading to the brain (De Chiara et al., 2019, Protto et al., 2024). TS was performed one/month up to 2 times. For dexamethasone treatment, the intraperitoneal injection was performed on the day of the TS-inducing virus reactivation and 24 hours later.

2.4. Stereotaxic surgery for LPS injection

For LPS injection, animals underwent stereotaxic surgery, as previously reported (Natale et al., 2024). Briefly, animals were anesthetized using a mixture of ketamine and xylazine (87.5 mg/Kg and 12.5 mg/Kg, respectively) and the skin above the skull was opened, after mounting the animal in the stereotaxic apparatus. Using a dental drill, a small craniotomy was performed. Five micrograms of LPS, diluted at 2μg/μL in a volume of 2.5 μL, were injected in each side at the following coordinates with respect to bregma: A.P. +1.2; M.L. ± 0.9; D.V. -3.9. Animals were then sutured and allowed to rest for a week before testing. For dexamethasone treated animals, the intraperitoneal injection was performed in the 30 minutes following the operation, as well as 24 hours later. FITC-conjugated LPS was injected to the same coordinates for diffusion evaluation (Supplementary Fig. 1A).

2.5. Immunofluorescence assays

To evaluate the inflammatory response, immunofluorescence analyses were performed on hippocampal and ventral striatum sections. Animals were overdoses on ketamine/xylazine cocktail and transcardially perfused with PBS followed by 4% paraformaldehyde solution. Coronal brain sections (30 μm thick) were obtained using a vibratome (Leica VT 1000S) and subsequently incubated for 1h at RT in a blocking solution containing 1% BSA, 0.5% Triton X-100 and 10% normal goat serum (NGS) in 0.1 M PBS. Then, samples were incubated overnight at 4°C with the following primary antibodies: Iba1 (1:200, Cat. No. #17198, Cell Signaling), TMEM119 (1:200, Cat. No. #98778, Cell Signaling), CD68 (1:200, Cat. No. #97778S Cell Signaling). After three washes in PBS, sections were incubated for 2h at RT with the appropriate secondary antibodies: Anti-rabbit IgG Alexa Fluor 488 (1:400, Cat.No #A-21206, Thermo Fisher Scientific) and Anti-mouse IgG Alexa Fluor 546 (1:400, Cat.No #A-10036, Thermo Fisher Scientific). Finally, the nuclei were counterstained with 4′,6-diamidino-2-phenylindole (DAPI, 0.5 μg/mL for 10 min, Invitrogen), and the slices were coverslipped with ProLong Gold anti-fade reagent (Invitrogen). Images (1024×1024) were acquired using a Nikon A1 MP confocal microscope with 20× and 60× objective lenses. ImageJ was used for cell counts.

2.6. Morphological analysis

For microglia morphological analysis, cells were labeled using the

Iba1-specific antibody. Iba1-positive cells in the VS were visualized using a Zeiss microscope with a motorized stage, connected to Neurolucida 7.5 (MicroBright-Field) software. Sholl analysis was performed to evaluate morphological complexity (Sholl, 1956). Specifically, the following structural parameters were quantified: (1) process length (μm); (2) the number of branch points (bifurcating nodes); (3) the number of terminal points of branches (endings); (4) the total number of intersections between a process and a shell; (5) cell soma perimeter and the surface area (Paciello et al., 2024).

2.7. Behavioural Assessment

Briefly, behavioural analyses were performed from 9:00 a.m. to 2:00 p.m. and data were collected and blindly analysed using the behavioural tracking system ANY-Maze™ (Stoelting Co., Wood Dale, IL, USA). For the 3 chambers social preference test (3CSPT), the apparatus (length = 58 cm, width = 40 cm, height = 20 cm) consisted of three interconnected chambers (19 × 40 × 20 cm each). The animals were first habituated, on day 1, for 10 minutes to the empty arena where empty upside-down wire cups were placed. The next day, under one of the cups, an inanimate object was placed, while a sex and age matched animal was placed in the other. Mice were then allowed to explore the arena for 5 minutes and time spent interacting with the mouse or the object was recorded. Then, the animal was removed from the arena for 30 minutes and the object was replaced with a novel mouse. At the end of the 30-minute interval, the animal was brought back into the apparatus and allowed to explore for 5 minutes, during which the interaction time between the mouse and the previously known or the new mouse was recorded. Preference indexes (PI) were then calculated: for the first phase (social vs. non-social stimulus), it was based on the ratio between time spent with the mouse and total time spent exploring the object and the mouse; for the second phase (new mouse vs. old mouse), it was based on the ratio between time spent exploring the new mouse and total time spent exploring both new and old mouse. For the novel object recognition (NOR) and object place recognition (OPR), animals were habituated for 10 minutes to an empty arena (33 x 33 cm). The next day, they were allowed to explore 2 identical objects for 5 minutes and, 30 minutes later, one of the objects was either replaced (NOR) or moved to a new position (OPR) and animals were allowed to explore for another 5 minutes. In the same way as in the social preference test, a preference index was computed as reported in previously published works (Rinaudo et al., 2022, Bandiera et al., 2024). For each test, the apparatus was cleaned with a 70% ethanol solution in between each animal. For the habituation/dishabituation task, animals were first habituated for 10 minutes to a square cage (33 x 33 cm) with empty holding cups. At the end of this interval, a same age, same sex conspecific was inserted inside the holding cup for 25 minutes, and exploration time was recorded and divided into 5 5-minutes blocks (0-5, 5-10, 10-15, 15-20, 20-25). Finally, for the last 5 minutes (20-25 block) a new animal was placed under the holding cup, removing the previous one. For all the behavioural tests involving social stimuli, a sex- and age-matched individual as an interactor was always employed.

2.8. Western blot analysis

Western blot analyses were performed as previously described (Natale et al. 2023). Hippocampal and striatal murine tissues were lysed in ice-cold lysis buffer (NaCl 150 mM, Tris-HCl 50 mM pH 8, and ethylenediaminetetraacetic acid (EDTA) 2 mM) containing 1% Triton X-100, 0.1% SDS, 1× protease inhibitor cocktail (Sigma-Aldrich), 1 mM sodium orthovanadate (Sigma-Aldrich), and 1 mM sodium fluoride (Sigma-Aldrich). Equal amounts of protein were diluted in a 6× Laemmli buffer, boiled, and resolved by sodium dodecyl-sulfate polyacrylamide gel electrophoresis (SDS-PAGE). Primary antibodies (available in SI Appendix, Table S1) were diluted 1:1,000 in TBS-T 3% milk (Biorad), incubated overnight, and revealed with horseradish peroxidase-conjugated secondary antibodies (Cell Signaling Technology Inc., Danvers, MA). Protein expression was evaluated and documented by UVItec Cambridge Alliance. Images shown were cropped for presentation with no manipulations. Full uncropped blots are reported in supplementary materials (See Suppl. Mat.).

2.9. Statistical analyses

Sample sizes were chosen with adequate power (0.8) according to results of prior pilot datasets or studies, including our own, that used similar methods or paradigms. Sample estimation and statistical analysis were performed using SigmaPlot 12 software. The statistical tests employed in the experiments (i.e., Student's *t* test, one-way Analysis of Variance (ANOVA), two-way ANOVA, Pearson correlation coefficient) and eventual post hoc multiple analyses are stated in the corresponding figure legends or relevant text. All statistical tests were two-tailed, and the level of significance was set at 0.05. Results are shown as mean ± SEM.

3. Results

3.1. HSV-1 induced neuroinflammatory shift within the VS.

Given the centrality of VS in modulating social behaviours, we first sought to investigate whether HSV-1 reactivation (Fig. 1A) could increase neuroinflammation in the microglial population within this region. One week after the second TS-induced reactivation, animals were sacrificed and Iba1 and TMEM119 immunostaining was performed along with analysis of Iba1-positive cell morphological changes in the VS (Fig. 1B). The number of Iba1-positive cells in HSV-1 infected animals was significantly higher compared to Mock-infected animals ($p=0.048$, Student's *t* test, Fig. 1C and D), although this was not accompanied by a significant reduction in microglial cells positive for both Iba1 and TMEM119 ($p=0.34$, Student's *t* test, Fig. 1C and E), a marker of homeostatic microglia (Mercurio et al., 2022). Concerning morphological alterations (Fig. 1F), HSV-1-infected mice showed a shift toward a pro-inflammatory phenotype, characterized by increased soma perimeter and area (perimeter: $p=0.012$, area: $p=0.002$, respectively, Student's *t* test, Fig. 1G, H), reduced number of intersections and nodes (intersections: $p=0.001$, nodes: $p<0.001$, respectively, Student's *t* test, Fig. 1I and J), reduced number of endings and reduced processes length ($p<0.001$ for both, Student's *t* test, Fig. 1K and L) compared to Iba1-positive cells from Mock-infected mice, thus indicating morphological features associated with an active microglia state in the VS of HSV-1-infected animals.

3.2. HSV-1 reactivation induces inflammatory-dependent social memory alterations.

We then sought to characterize whether HSV-1 reactivation could induce social memory alterations and whether these effects could be dampened by broad anti-inflammatory treatment. To this end, Mock- and HSV-1-infected mice were treated with intraperitoneal injections of vehicle solution or dexamethasone solution (5 mg/Kg), during the reactivation procedure and 24 hours after it. One week after the 2TS, a time point where we have previously demonstrated that HSV-1-infected animals start to show behavioural and synaptic plasticity abnormalities (Li Puma et al., 2023), animals underwent the 3CSPT. In all four groups we did not observe any variations in the preference index for the social stimulus compared with the non-social stimulus ($p<0.001$ for all; Student's *t* test, Fig. 3B). However, when assessing social memory, HSV-1-infected mice showed no significant difference between novel and old mouse, an effect that was reversed by dexamethasone treatment (HSV-1 + Vehicle, Old Mouse vs. New Mouse: $p=0.938$; HSV-1 + Dexamethasone, Old Mouse vs. New Mouse: $p=0.003$, Student's *t* test, Fig. 2C), while both Mock-conditions showed a significant preference for the

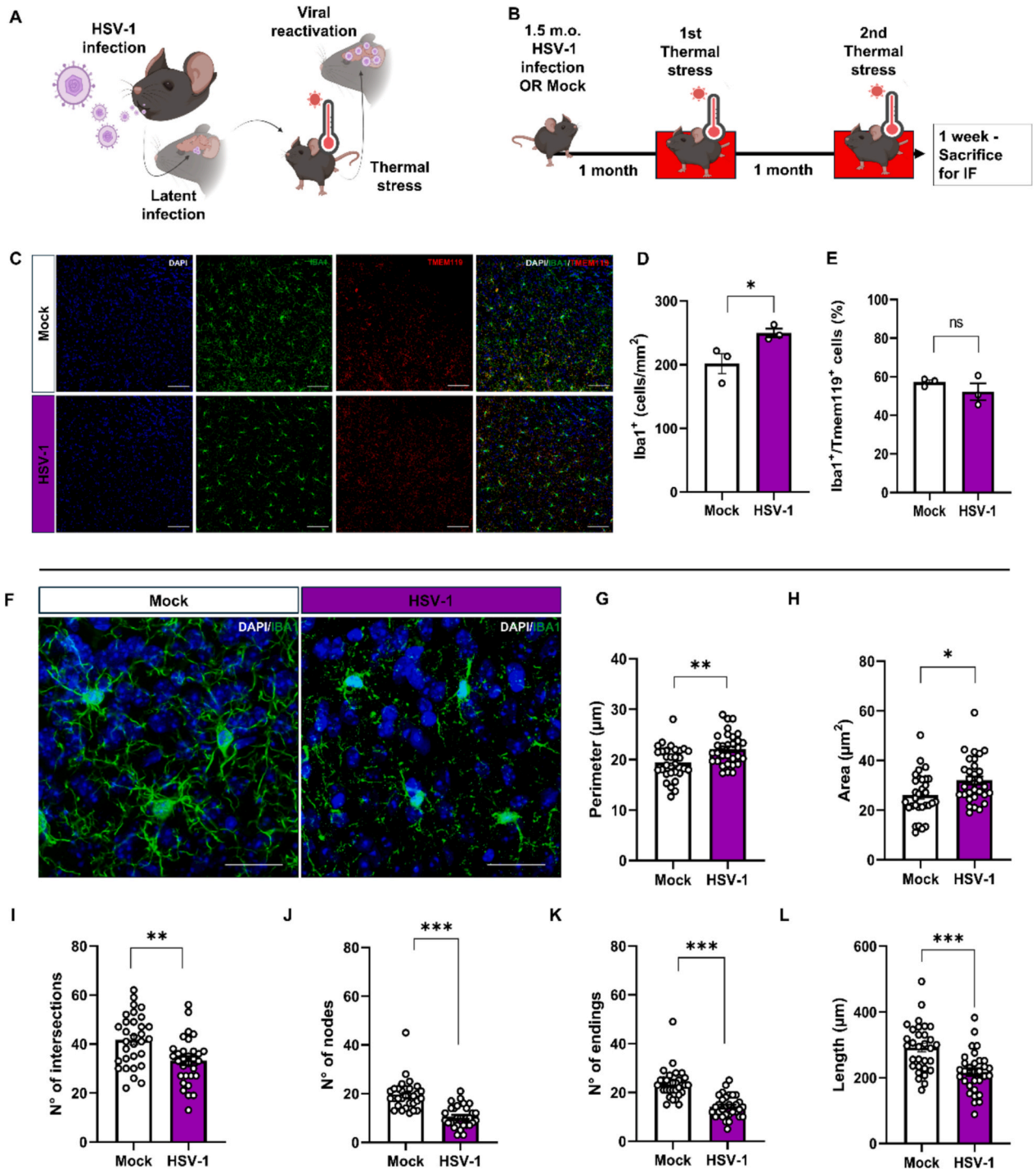

Fig. 1. HSV-1 induces neuroinflammation in the ventral striatum. A and B) Experimental procedure and timeline of HSV-1 infection and reactivation. C) Representative confocal images of Iba1 and TMEM119 immunostaining in the VS. D–E) Quantification of total Iba1$^+$ and Iba1$^+$/TMEM119$^+$ microglia cells. Scale bar: 100 µm; Mock-infected animals (Mock) n = 3, HSV-1-infected animals (HSV-1) n = 3. F) Representative immunofluorescence images showing Iba1 staining in Mock and HSV-1 animals. G–L) Histograms showing soma morphological analysis and branching complexity of Iba1-stained cells; n = 31 cells from 3 Mock animals and n = 31 cells from 3 HSV-1 mice. Statistics by unpaired Student's *t* test. Scale bar: 25 µm. Data are reported as mean ± SEM. *p < 0.05; **p < 0.01; ***p < 0.001; ns = not significant.

novel mouse (Mock + Vehicle, Old Mouse vs. New Mouse: p=0.007; Mock + Dexamethasone, Old Mouse vs. New Mouse: p=0.014, Student's *t* test, Fig. 2C). Overall, these data indicate that HSV-1 reactivation induces inflammatory-dependent alterations in social short-term memory.

3.3. Ventral striatum intracerebral injections of LPS induces localized inflammatory responses and striatal synaptic alterations.

Previously published works from our group demonstrate that the HSV-1 model is characterized by broad neuroinflammatory alterations in different brain regions such as cortical areas and hippocampus, making it difficult to identify whether the specific behavioural

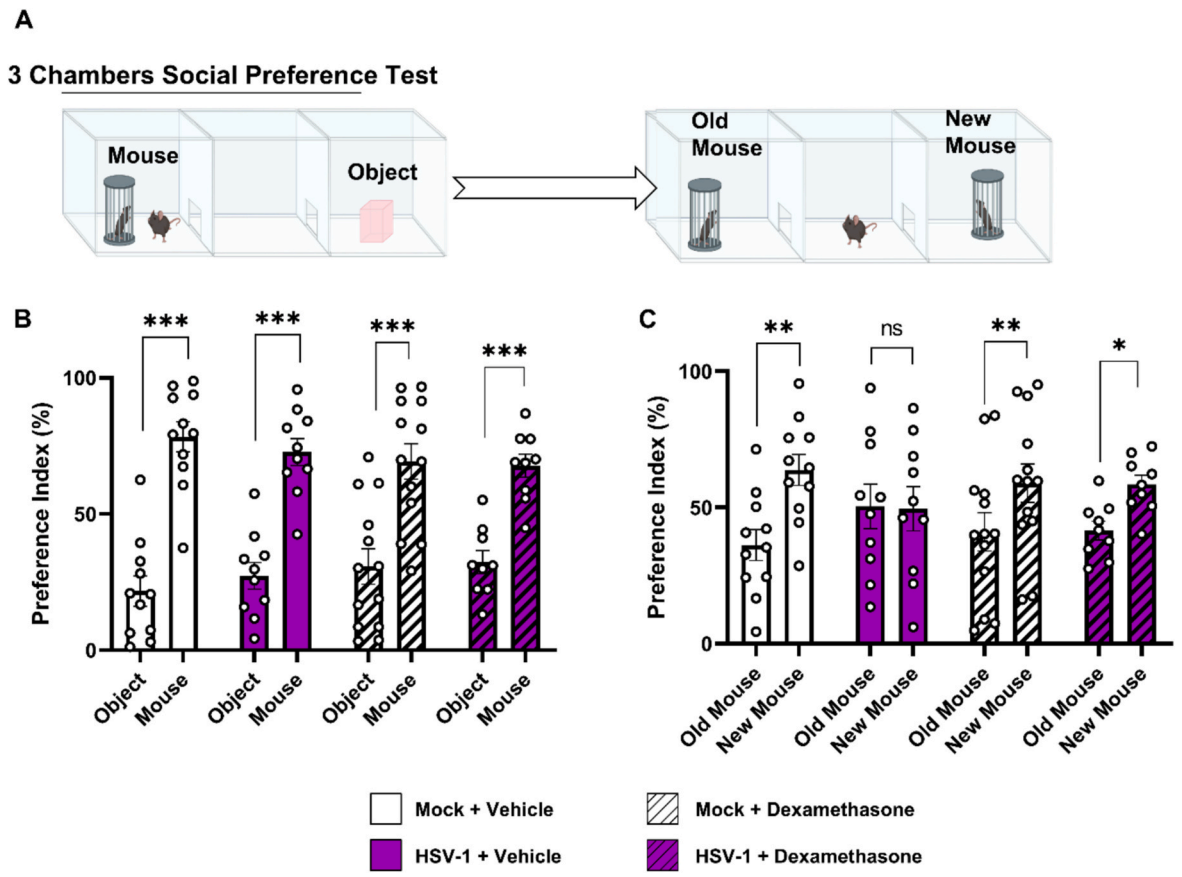

Fig. 2. HSV-1 induces neuroinflammatory-dependent deficits in social behaviour. A) Schematic representation of the 3CSPT. B-C) Preference indexes for social vs. non-social stimuli (B) and known and unknown mouse (C) HSV-1 recurrency induces an impairment in social memory, which is rescued by dexamethasone treatment. Statistics by unpaired Student's *t* test; n = 9–13 animals per group. Data are reported as mean ± SEM. *p < 0.05; **p < 0.01; ***p < 0.001; ns = not significant.

alterations we observed depend on alterations specifically of the VS. Therefore, we employed a different approach to obtain a more localized and controlled inflammatory response through LPS intracerebral injection directed at the VS. Mice were stereotaxically operated and received 5 μg of LPS per side (Fig. 3A). One week after the injection, animals were sacrificed and the hippocampus and VS were collected for molecular analyses. We first evaluated the levels of pro-inflammatory signalling molecules, such as phosphorylation of STAT3 and NF-kB, in the VS and hippocampus. In the VS, LPS-injected animals showed significantly higher levels of STAT3 phosphorylation at Tyr705 (Saline vs. LPS p=0.023, Student's *t* test, Fig. 3B, C), a significant increase in total STAT3 levels (Saline vs. LPS p=0.001, Student's *t* test, Fig. 3B, C) and heightened NF-kB Ser536 phosphorylation (Saline vs. LPS p=0.003, Student's *t* test, Fig. 3B, C). Regarding synaptic plasticity markers, LPS-injections induced a significant increase in GluA2 levels (Saline vs. LPS p=0.032, Student's *t* test, Fig. 3B, C). No differences were observed in total PSD-95 levels (Saline vs. LPS p=0.945, Student's *t* test, Fig. 3B, C), as well as in the phosphorylation at Ser845 of GluA1 (Saline vs. LPS p=0.569, Student's *t* test, Fig. 3B, C), suggesting that the number of synapses may have not been impacted but, instead, synapse receptor composition. Of note, the same inflammatory markers in the hippocampus were not significantly affected by VS LPS-injection (STAT3 Tyr705: Saline vs. LPS p=0.473, Student's *t* test, Fig. 3D, E; NF-kB Ser536: Saline vs. LPS p=0.998, Student's *t* test, Fig. 3D, E), thus suggesting that the inflammatory response was region confined.

3.4. Dexamethasone is sufficient to halt LPS-induced social memory alterations.

Once defined the spatial neuroinflammatory boundaries of VS-LPS injection, we evaluated its impact at the behavioural level and whether LPS detrimental effects could be halted by dexamethasone treatment. Again, to confirm the specificity of our model, animals were first evaluated in the NOR and OPR tests, which assess object and spatial short-term memory, which are not directly dependent from the VS (Fig. 4A). Indeed, LPS-injected mice did not show any alterations in object or spatial memory (LPS: Old Object vs. New Object, p=0.001, Student's *t* test, Fig. 4B ; LPS: Stationary Object vs. Displaced Object, p<0.001, Student's *t* test, Fig. 4C), with performances being on par with vehicle-injected animals (Saline: Old Object vs. New Object, p<0.001, Student's *t* test, Fig. 4B ; Saline: Stationary Object vs. Displaced Object, p<0.001, Student's *t* test, Fig. 4C). We then sought to determine the extent of social memory deficits induced by intra-VS injection of LPS (Fig. 4D). First, to exclude potential confounders due to altered social reward processes, we performed a social habituation/dishabituation. In the habituation/dishabituation task, two-way ANOVA on Time × Treatment revealed a significant effect of LPS injection (LPS: $F_{(4, 52)}$=6.168, p=0.027, Fig. 4D) and a significant effect of Time (Time: $F_{(2.227, 28.95)}$ = 29,47; p<0.001, Fig. 4D).When the new mouse was introduced, both Saline- and LPS-injected mice showed a significant increase in exploration time compared to the last block of exploration (Sidak's multiple comparison test, 15-20 block vs. 20-25 block: Saline: p=0.028; LPS: p=0.024, Fig. 4D). In the 3CSPT, LPS-injected animals showed no preference for their conspecific compared to the object-stimulus in the training phase (LPS: Object vs. Mouse, p=0.338,

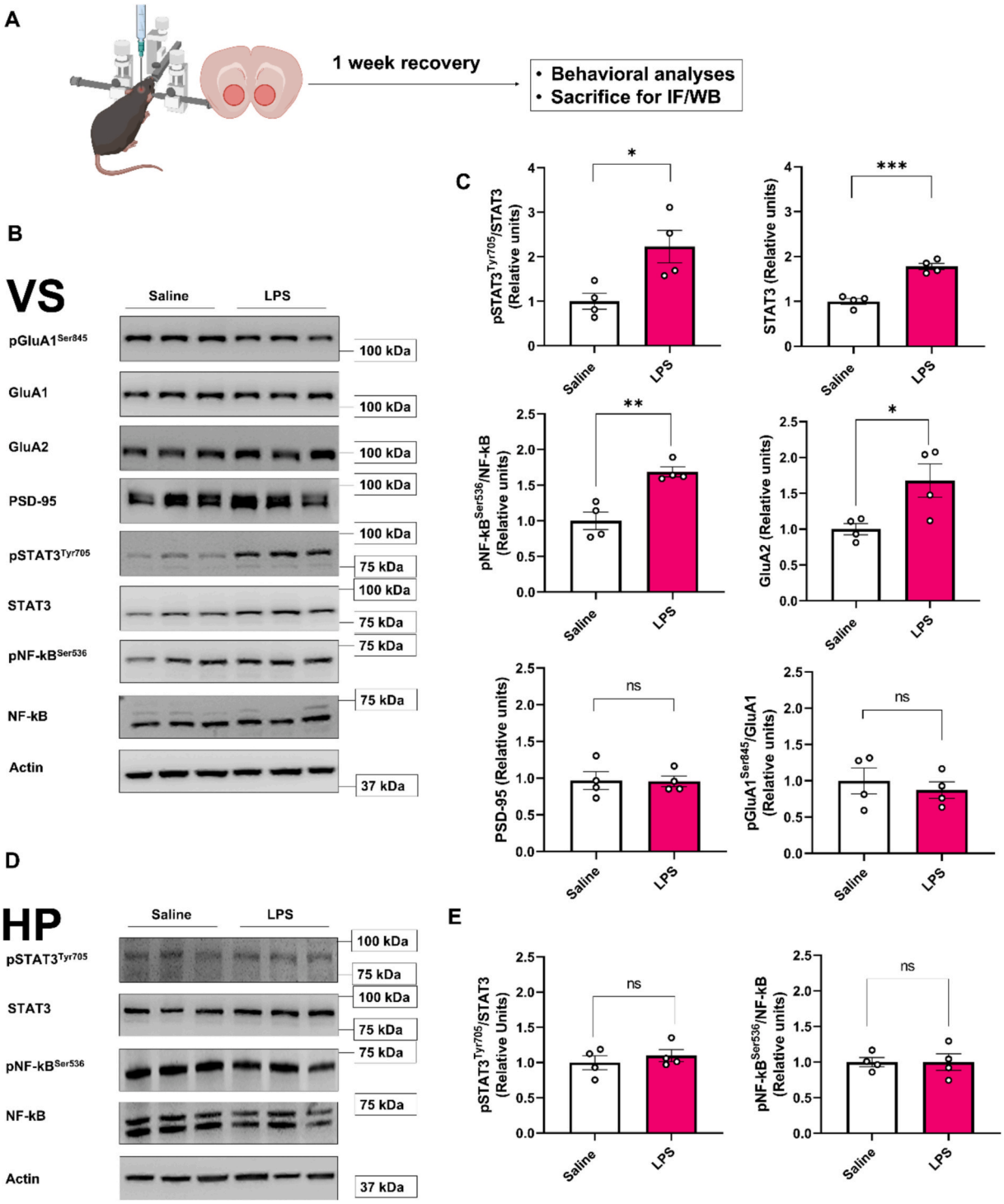

Fig. 3. LPS intracerebral injection induces localized neuroinflammatory reactions. A) Schematic representation of the injection paradigm. B and C) Representative blots from VS and associated densitometric analyses. D and E) Representative blots from HP and associated densitometric analyses. Results indicate that in the VS there is an increase in neuroinflammatory markers accompanied by GluA2-dependent synaptic remodelling; on the other hand, in the hippocampus of the same mice, no differences were observed in the phosphorylation levels of STAT3 or NF-kB. Statistics by unpaired Student's *t* test; n = 4 animals per group. Data are reported as mean ± SEM. *p < 0.05; **p < 0.01; ***p < 0.001; ns = not significant.

Student's *t* test, Fig. 4E). and did not show any preference for the new mouse compared to the old mouse, which was, on the contrary, the preferred one (LPS: Old Mouse vs. New Mouse, p=0.041, Student's *t* test, Fig. 4F). Dexamethasone treatment was able to revert both effects (LPS + Dexamethasone: Object vs. Mouse, p<0.001, Student's *t* test, Fig. 4G; LPS + Dexamethasone: Old Mouse vs. New Mouse, p<0.001, Student's *t* test, Fig. 4H). When directly comparing the preference index for the old and new mouse, we observed a net effect of Treatment (Old/New: Treatment: $F_{(1,\ 36)}$= 17.82; p<0.001; Two-Way ANOVA, Fig. 4G and H), of LPS (LPS-injection: $F_{(1,\ 36)}$=17.60; p<0.001; Two-Way ANOVA, Fig. 4G and H) and a significant effect of interaction (Treatment × LPS-injection: $F_{(1,\ 36)}$=5.599; p=0.023; Two-Way ANOVA, Fig. 4G and H). Post-hoc analyses revealed that the preference index for the novel or old mouse was significantly lower and higher, respectively, compared to all

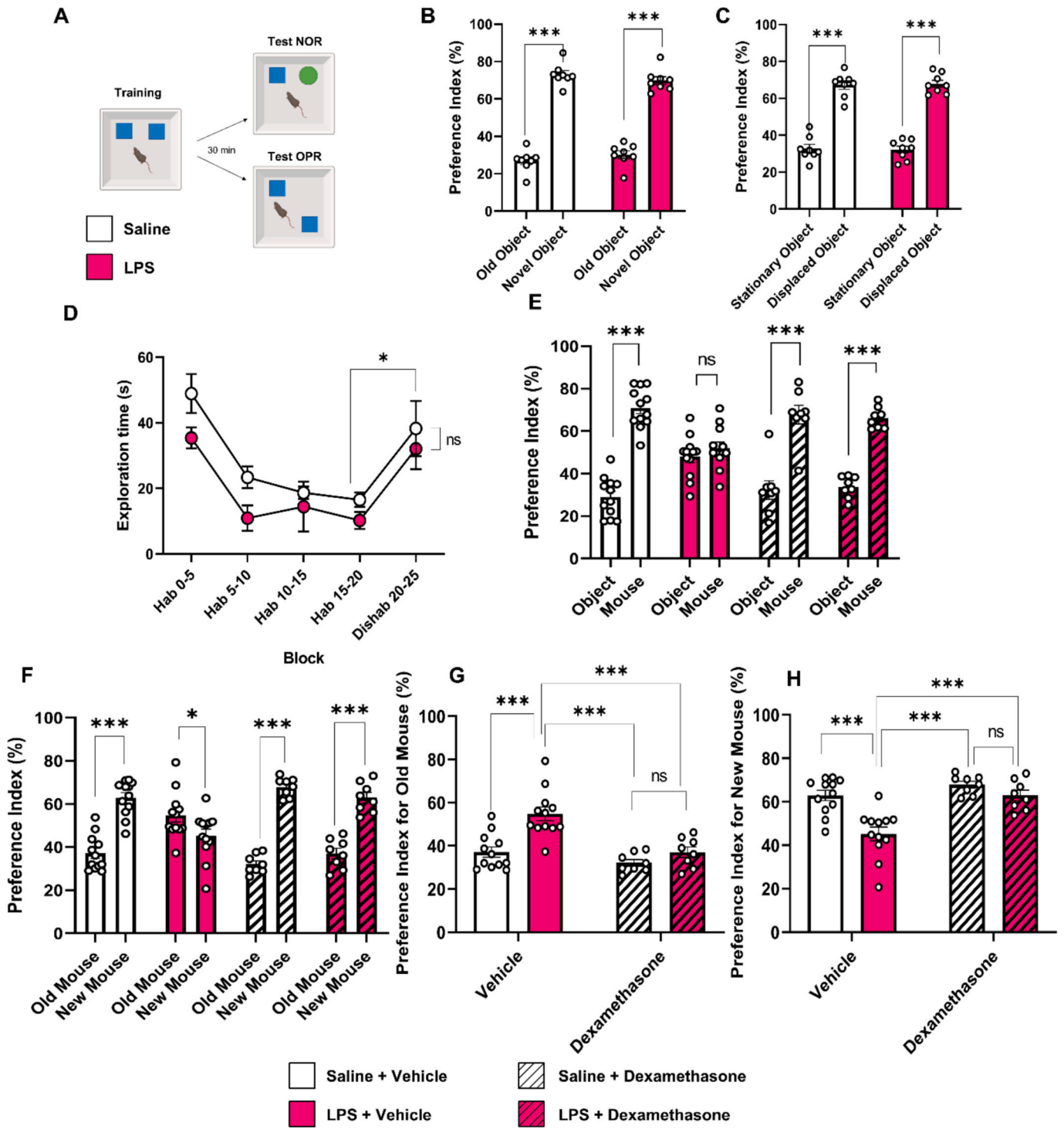

Fig. 4. LPS intracerebral injection induces neuroinflammatory-dependent social memory alterations. A) Schematic representation of the NOR and OPR paradigms. B and C) LPS-injected mice show overlapping recognition and spatial memory performances in both tests, thus suggesting localized damage to extra-hippocampal structures. D) Habituation/Dishabituation task, showing similar habituation curves for both Saline and LPS injected animals. E to H) Preference indexes in the 3CSPT. LPS-injected mice show a reduction in the PI for the mouse, and a significant preference for the old/known mouse. Preference indexes for the new and old mouse in LPS-injected mice were significantly different from all other conditions. All the effects were reversed by dexamethasone treatment. Statistics by two-way ANOVA and Student's *t* test; n = 8–12 animals per group. Data are reported as mean ± SEM. *p < 0.05; ***p < 0.001; ns = not significant.

other conditions (LPS+Vehicle vs. Saline + Vehicle: p<0.001; vs. Saline + Dexamethasone: p<0.001; vs. LPS + Dexamethasone: p<0.001; Fig. 4G and H) thus suggesting impaired social memory.

3.5. *Dexamethasone partially counteracts inflammatory profiles in LPS-injected animals.*

We then sought to characterize the extent of the pro-inflammatory shift in the VS of LPS-injected mice, in the presence and absence of dexamethasone and evaluate if some specific parameters in macrophage

morphology could differentially correlate with behavioural performances. Again, we performed Iba1, TMEM119 and CD68 staining as well as microglial morphological analyses. LPS injection increased the number of Iba1 positive cells (LPS injection: $F_{(1,\ 12)}=45.64$, $p<0.001$, two-way ANOVA, Fig. 5A and B) along with a decrease in Iba1/TMEM119 double positive cells (LPS injection: $F_{(1,\ 12)}=13.65$, $p<0.003$, two-way ANOVA, Fig. 5A and C); this increase was observed only in the VS but not in the hippocampus (Fig. 6A, B and C), further confirming the localized nature of neuroinflammation. Dexamethasone treatment reverted Iba1 counts (Treatment: $F_{(1,\ 12)}=9.39$, $p=0.009$, Fig. 5B) while Iba1/TMEM119 showed a trend toward increase ($F_{(1,\ 12)}=4.515$, $p=0.055$, two-way ANOVA, see Fig. 5C for post-hoc comparisons). Since different reports have shown that TMEM119 is a homeostatic marker which is not necessarily downregulated during inflammation (Ruan and Elyaman, 2022), we also assessed the number of CD68+ cells in VS, which is a marker of phagocytic/lysosomal activity (Lier et al., 2021). Immunofluorescence analysis revealed that LPS induced a significant increase in $CD68^+/Iba1^+$ cells in the VS ($F_{(1,\ 12)}=27.09$, $p<0.001$,

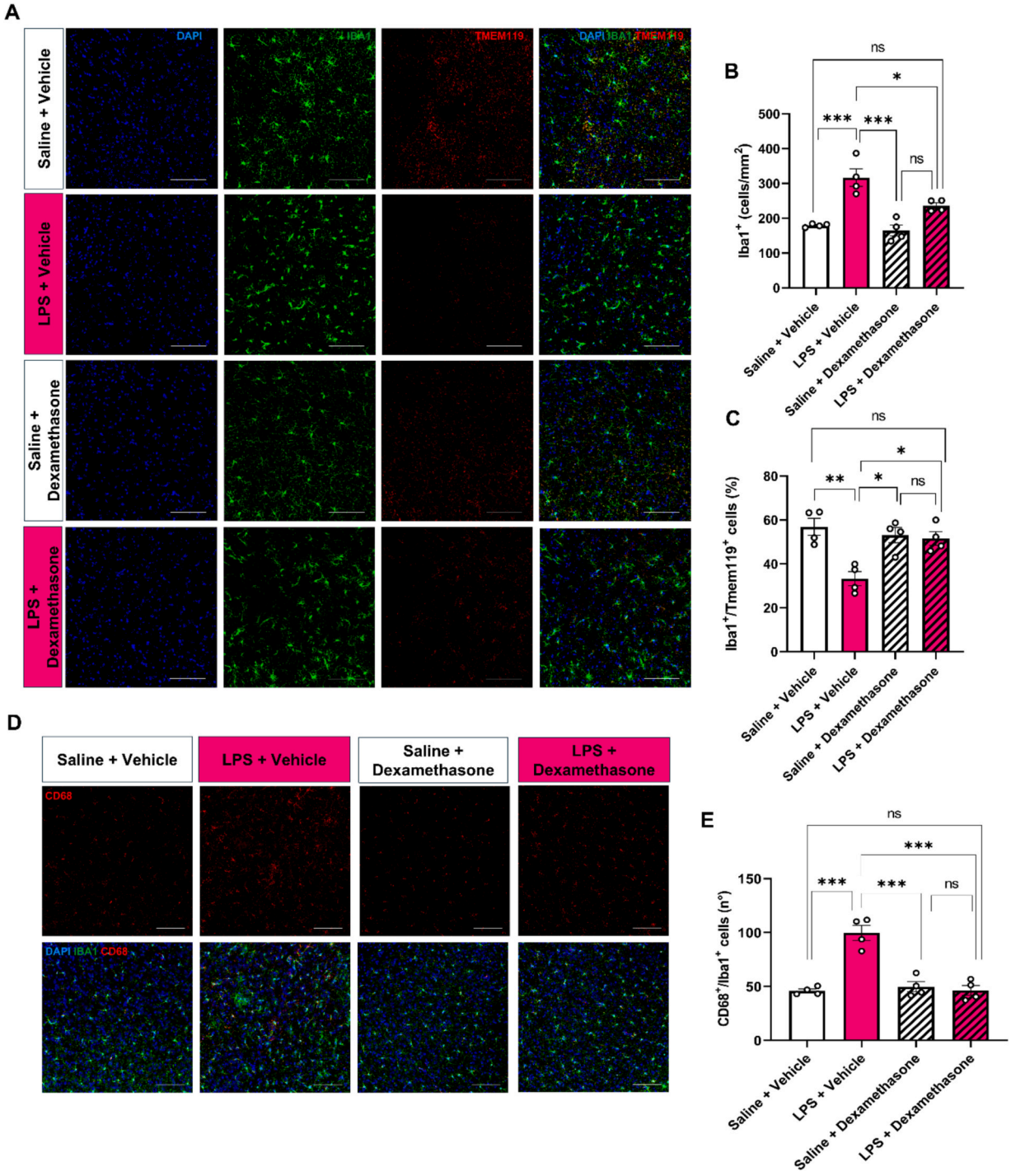

Fig. 5. Dexamethasone counteracts LPS-induced neuroinflammation in the VS. A) Representative confocal images of Iba1 and TMEM119 immunostaining in the VS. B and C) Quantification of total $Iba1^+$ cells and $Iba1^+/TMEM119^+$ microglia. D and E) Representative confocal images of $Iba1^+/CD68^+$ cells followed by quantification. Both $Iba1^+$ cells, $Iba1^+/TMEM119^+$ ratio and $Iba1^+/CD68^+$ cells were normalized by dexamethasone treatment. Statistics by two-way ANOVA; n = 4 animals per group. Data are reported as mean ± SEM. *p < 0.05; **p < 0.01; ***p < 0.001; ns = not significant. Scale bar: 100 μm.

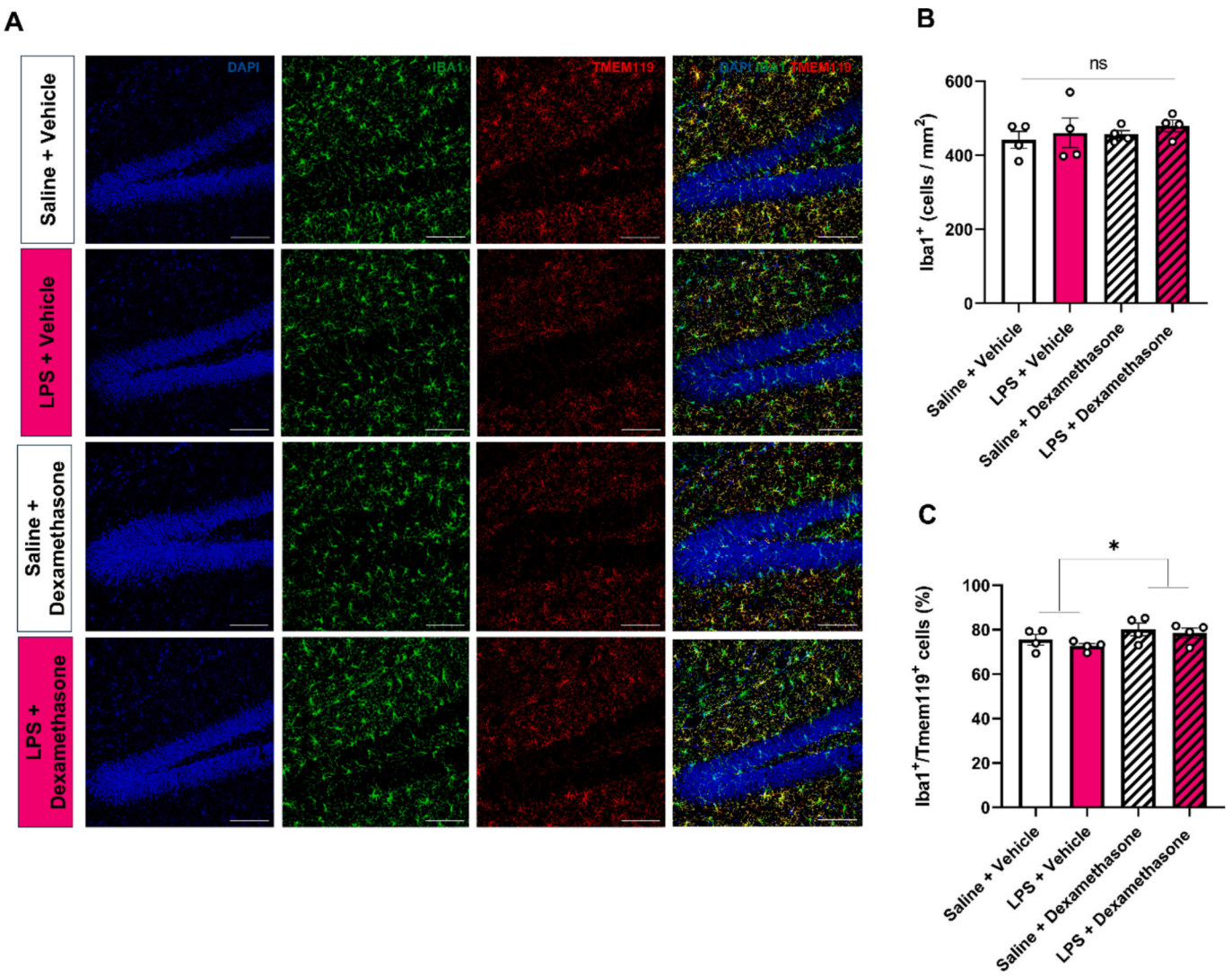

Fig. 6. VS-LPS injection does not induce increase in Iba1 staining in the dentate gyrus of the hippocampus while increasing TMEM119 immunoreactivity. A) Representative confocal images of Iba1 and TMEM119 immunostaining in the dentate gyrus of the hippocampus. B and C) Quantification of total Iba1$^+$ cells and Iba1$^+$/TMEM119$^+$ microglia. Statistics by two-way ANOVA; n = 4 animals per group. Data are reported as mean ± SEM. *p < 0.05; ns = not significant. Scale bar: 100 μm.

Fig. 5D and E) and dexamethasone treatment reverted this condition ($F_{(1, 12)}$=26.07; p<0.001, Fig. 5E). Of note, we observed a net effect of dexamethasone in the hippocampus in increasing the percentage of Iba1/TMEM119 positive cells without impacting total number of Iba1 (Treatment: $F_{(1, 12)}$=5.415, p=0.038; two-way ANOVA, Fig. 6B and C). Regarding microglial morphological analysis (Fig. 7A and B), LPS induced a drastic shift toward an amoeboid phenotype in the VS, significantly reducing branching complexity and increasing soma perimeter and area (LPS vs. Saline factor: Perimeter: $F_{(1, 123)}$=24.41, p<0.001; Area: $F_{(1, 123)}$=15.95, p<0.001; Nodes: $F_{(1, 123)}$=210.5, p<0.001; Intersections: $F_{(1, 123)}$=202.5, p<0.001; Length: $F_{(1, 123)}$=210.5, p<0.001; Endings: $F_{(1, 123)}$=88.64, p<0.001; two-way ANOVA, Fig. 7A-H). Dexamethasone treatment did not significantly revert most of the morphological features of the pro-inflammatory shape, although the number of nodes and number of endings in dexamethasone-treated animals were significantly different from vehicle-treated mice (Vehicle vs. Dexamethasone factor: Perimeter: $F_{(1, 123)}$=2.274, p=0.134; Area: $F_{(1, 123)}$=2.335, p=0.129; Nodes: $F_{(1, 123)}$=210.5, p<0.001; Intersections: $F_{(1, 123)}$=1.507, p=0.220; Length: $F_{(1, 123)}$=3.524, p=0.0629; Endings: $F_{(1, 123)}$=37.16, p<0.001; two-way ANOVA, Fig. 7C-H). A significant effect of interactions was observed for multiple morphological parameters (Perimeter: $F_{(1, 123)}$=0.001, p=0.970; Area: $F_{(1, 123)}$=0.221, p=0.638; Nodes: $F_{(1, 123)}$=19.96, p<0.001; Intersections: $F_{(1, 123)}$=18.17, p<0.001; Length: $F_{(1, 123)}$=19.96, p<0.001; Endings: $F_{(1, 123)}$=35.00, p<0.001; two-way ANOVA, Fig. 7C-H). Post-hoc comparisons showed that LPS + Dexamethasone condition was always significantly different from Saline + Vehicle/Dexamethasone, except for area (Saline + Vehicle vs. LPS + Dexamethasone: p=0.302; Saline + Dexamethasone vs. LPS + Dexamethasone: p=0.064; Tukey's multiple comparison, Fig. 7D) and endings (Saline + Dexamethasone vs. LPS + Dexamethasone: p=0.067; Tukey's multiple comparison, Fig. 7H). Of note, dexamethasone treatment itself induced a general morphological shift toward a more amoeboid phenotype, except for area and perimeter parameters (Tukey's multiple comparisons, see Fig. 7C to H), thus suggesting that it's main contribution could be more related to the reduction of immune cells recruitment to the VS in response to the inflammatory stimulus.

Finally, we assessed whether inflammatory profiles in the VS and dorsal hippocampus could be directly correlated to the behavioural performances. As shown in Fig. 8, we correlated all the inflammatory parameters assessed through immunofluorescence and morphological analyses with behavioural parameters assessed in the 3CSPT. In the VS,

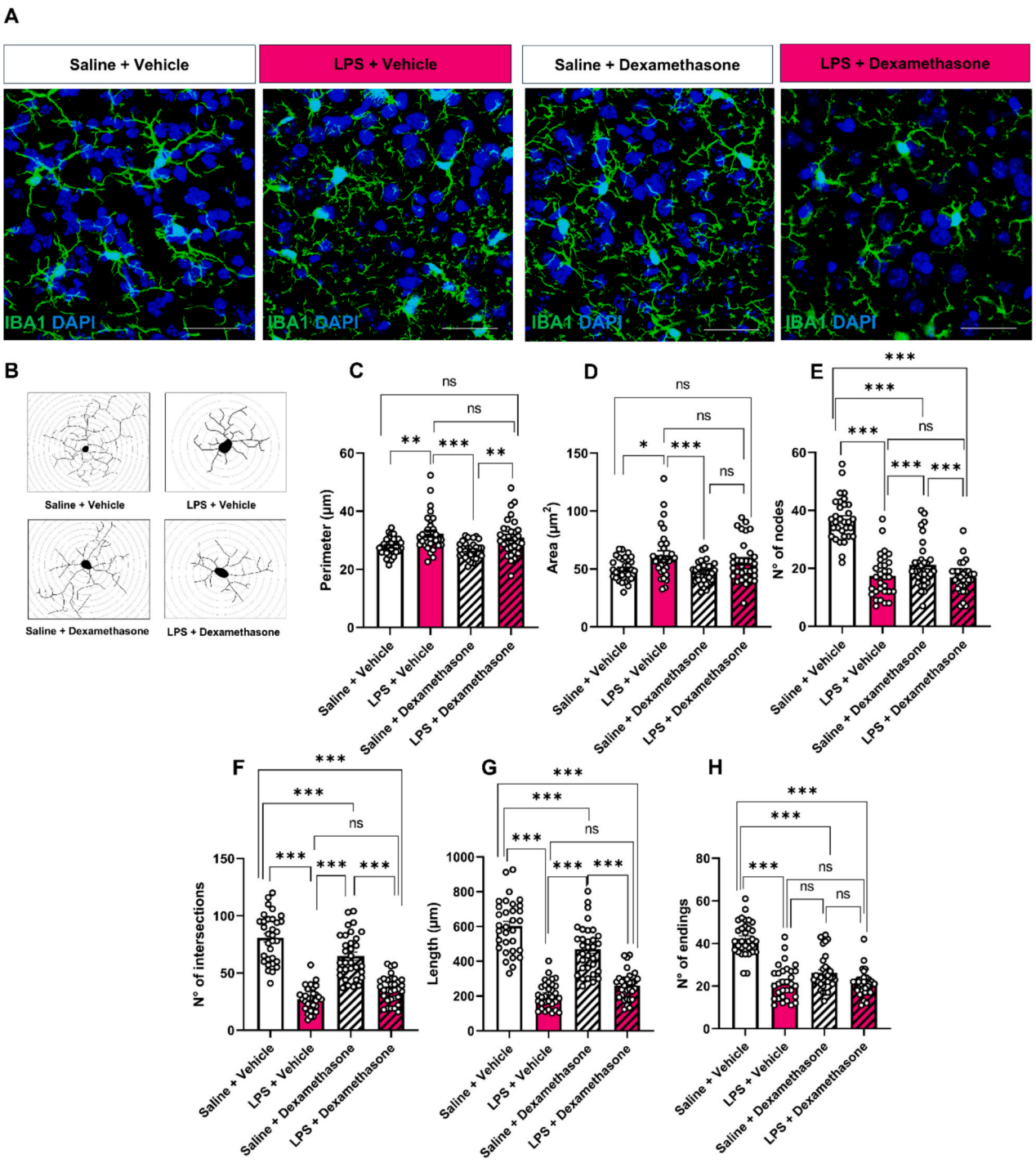

Fig. 7. Dexamethasone induces partial recovery of microglial morphology in the VS. A) Representative confocal images of Iba1 and TMEM119 immunostaining. B) Representative camera lucida drawings of Iba1 stained cells with Sholl analysis. C–H) Quantification of soma size and branching complexity. Statistics by two-way ANOVA; n = 31–32 cells per condition from 4 animals per group (6–10 cells analysed per animal). Data are reported as mean ± SEM. *p < 0.05; **p < 0.01; ***p < 0.001; ns = not significant. Scale bar: 25 µm.

although some microglial morphology parameters almost reached a significant correlation with behavioural parameters, such as microglial area, soma perimeter as well as total processes length (Fig. 8A), the only significant correlations that we observed were between the percentage of Iba1$^+$/TMEM119$^+$ cells and time spent exploring the social stimulus in the object-mouse phase, and between the number of Iba1$^+$ cells and time spent exploring the known mouse in the test phase of the 3CSPT, which were, in both cases, positively correlated (Mouse exploration in object-mouse phase: Pearson's r=0.530, p=0.035; Old mouse exploration in new-old mouse phase: Pearson's r=0.520, p=0.039, Fig.8B and C). Regarding hippocampal dentate gyrus, correlation heatmap is shown in Fig. 8D. Of note, the percentage of Iba1/TMEM119 positive cells from the dentate gyrus of the dorsal hippocampus significantly correlated with social memory indexes in the 3CSPT (Pearson's r=-0.614 for PI Old Mouse, r=0.614 for PI New Mouse, p= 0.011, Fig. 8E) as well as with time spent exploring the old mouse (Old Mouse exploration: Pearson's r=-0.508, p=0.044, Fig. 8F) therefore confirming a role for the dorsal hippocampus in social memory while suggesting a

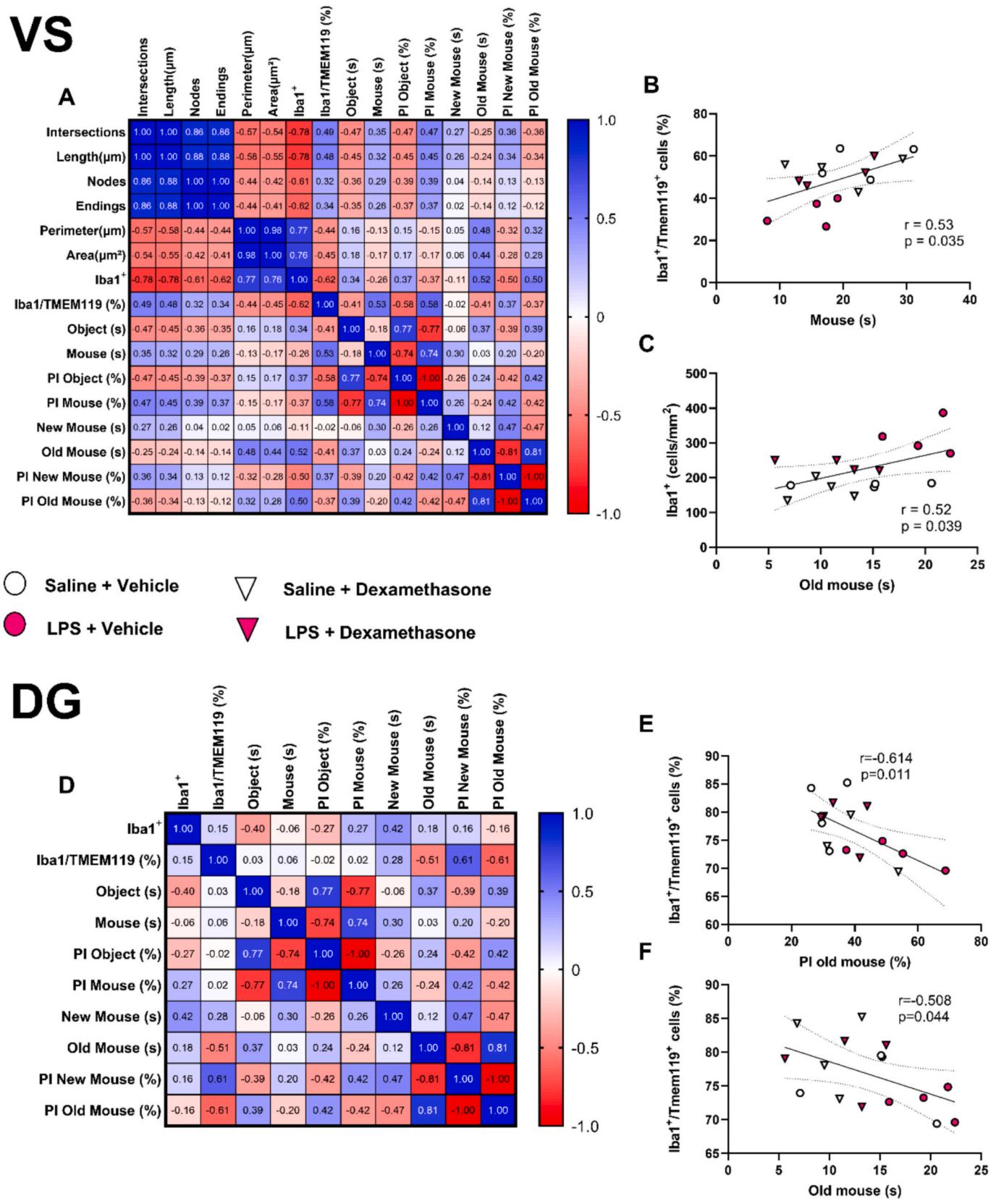

Fig. 8. VS-Iba1^{+} cells number and TMEM119 expression is associated with time spent exploring the old mouse. A) Correlation heatmap between the microglial parameters assessed in the VS and behavioural performance. B and C) Significant correlation was observed between the percentage of Iba1/TMEM119 positive cells and time spent interacting with the conspecific in the object-mouse phase, while Iba1 number correlated with time spent exploring the Old Mouse in the test phase of the 3CSPT. D, E and F) A similar pattern was observed in the dentate gyrus of the hippocampus, where homeostatic microglia was associated with better memory performance.

role for VS inflammatory signalling in gating the expression of social memory, as the higher the number of Iba1-positive cells in the VS, the higher the time spent exploring the known stimulus.

4. Discussion

Neuroinflammatory processes are complex responses impacting multiple brain processes, ranging from mood regulation, cognitive abilities as well as social functions. Increased inflammation has been associated with both neurodegenerative and neuropsychiatric disorders, through alterations induced in synapse structure and function followed by heavy circuit remodelling and neurodegeneration (Zhang et al., 2023). In the context of social behaviour, neuroinflammatory stimuli can induce extremely nuanced behaviours, ranging from avoidance to social approach, depending on a plethora of factors, such as gender, type of inflammatory stimulus or familiarity with the conspecific as well as timing of social behaviour assessment (Moieni and Eisenberger, 2018).

LPS has been widely used to generate systemic inflammation impacting also on brain function. Peripheral LPS injection induces anxiety and social withdrawal, cognitive deficits, as well as alterations in synaptic transmission in NAc, amygdala or prefrontal cortex (Zhang et al., 2022, Sheppard et al., 2019). LPS-injection in humans presented with either familiar people or complete strangers elicits an increase in the desire to be around familiar stimuli, relative to placebo-injected controls. These feelings were associated with higher BOLD signal in the dopaminergic striatum, which was also directly correlated to the interleukin 6 response (Inagaki et al., 2015, Lohrenz et al., 2016). Similar findings were also observed in rhesus monkeys, rats and prairie voles (Willette et al., 2007, Yee and Prendergast, 2010, Bilbo et al., 1999). Our results show that, while responsiveness to social novelty is maintained, VS neuroinflammation is sufficient to alter social memory, as shown by direct comparison of memory performance between all conditions assessed. Furthermore, LPS treatment promoted a small, although statistically significant, preference for the known mouse, a phenomenon that correlated with the number of Iba1^{+} cells in the VS, and that is in line with previously described findings. Of note, VS Iba1/TMEM119 signals correlated with time spent exploring the social stimulus in the first phase of the 3CSPT, reflecting the role of VS in regulating social approach/avoidance. Hippocampal Iba1/TMEM119 signal correlated with memory, as expected, thus suggesting that, while the hippocampus is involved in memory and novelty discrimination through pattern-separation mechanisms, neuroinflammatory signalling in the VS may bias memory retrieval toward familiar stimuli even in the presence of a functional hippocampus. Indeed, in the HSV-1 model, we did observe disrupted social memory, along with no preference for the old mouse. As we have previously demonstrated, HSV-1-infected and reactivated mice are characterized by widespread brain inflammation, reaching also the hippocampus (Li Puma et al., 2019), and literature reports have shown that neuroinflammatory processes in the hippocampus can disrupt different types of memory (Yong et al., 2021). It is possible therefore that, when both the hippocampus and VS are subjected to neuroinflammation, hippocampal dysfunction doesn't allow memory retrieval at all, independently from VS gating of memory expression. Indeed, information flow within the dCA2-vCA1-NAc circuit support the role of VS in weighing internal signals and relaying this information to decisional areas, such as the mPFC, biasing the behavioural output toward a specific strategy, such as avoiding novel conspecifics or preferring known social stimuli (Li et al., 2025, Okuyama et al., 2016).

LPS induced an increase in the levels of STAT3 and NF-kB phosphorylation in the VS even at one week after the injection, a phenomenon that was not mirrored in the hippocampus. Indeed, sustained inflammation could explain the shift of AMPA receptors composition within the VS in regulating social memory expression, as an increase in calcium-impermeable AMPA subunits may indicate fewer plastic synapses at the level of vCA1-NAc projections (Kopach et al., 2011, DiSabato et al., 2016, Kawasaki et al., 2008). Microglial activity may act as an upstream driver of these changes, given its established role in releasing cytokines that regulate AMPAR trafficking, spine stability, and glutamatergic tone but also dopaminergic or serotonergic release, which have been shown to be heavily involved in the expression of social memory (Padilla-Coreano and Martínez-Rivera, 2025, Zorab et al., 2025).

Systemic dexamethasone treatment was able to reduce the number of Iba1^{+} cells, and to restore the ratio of Iba1/TMEM119 positive cells in the VS, along with reduced number of CD68/Iba1 positive cells. Multiple lines of evidence indicate that dexamethasone fails to penetrate the blood-brain barrier due to the activity of mdr1a protein (Meijer et al., 1998), although dexamethasone has been the staple glucocorticoid analogue for the last 60 years in neurosurgery, with great success, for treatment of brain inflammation and oedema after stroke or after surgery (Vazquez et al., 2023). Dexamethasone can have also systemic effects, due to it triggering glucocorticoid cascade, and had its own impact on social behaviours: beside inducing a recovery of function in the 3CSPT in both models, it also impacted macrophage abundance in the hippocampus as well as Iba1-positive cells morphology in the ventral striatum (Park et al., 2019). However, dexamethasone treatment did not induce a recovery in macrophage morphology in the VS of LPS-injected animals. Non-resident immune cells may transmigrate within the central nervous system to respond to the neuroinflammatory insult: however, the direct relationship between peripheral surveillance of central processes in the manifestation of complex functions such as social behaviour or memory is still unclear (Kopec et al., 2019). Recent evidence indicates that lateralized lesions of dopaminergic neurons within the VS can impair immune cell proliferation and natural killer cell activity in the spleen, suggesting a bidirectional connection between the immune system and the VS (Deleplanque et al., 1994, Ben-Shaanan et al., 2016). In this context, we speculate that dexamethasone may have shunted the inflammatory response of peripheral immune cells and reduced their entrance within the CNS, therefore halting their direct contribution to synapse remodelling within the VS.

Neuroinflammation induced from peripheral or central stimuli, has been also associated with loss of dopaminergic projection to striatal neurons from the substantia nigra (SN) and/or ventrotegmental area (VTA, Brown, 2019). Indeed, different reports have characterized LPS-induced nigrostriatal loss of dopaminergic terminals. In one striking and unfortunate case, a laboratory worker came into contact, through an open wound, with LPS from *Salmonella minnesota*. This led, in a time span of a few weeks, to the development of Parkinson's Disease symptoms, characterised by tremor and rigidity and, in the following years, by the accumulation of synuclein aggregates within the SN (Liu and Bing, 2011). Previous works have demonstrated that direct injections of LPS within the striatum induce progressive dopaminergic loss, generating both motor and cognitive symptoms (Beier et al., 2017). Indeed, it is possible that, in both of our models, monoaminergic terminals may have been among the main targets of the aggressive immune response. Recent evidence has demonstrated that in the early phases of Alzheimer's Disease (AD), there is a strong loss of VTA projection neurons in both transgenic mouse models and in human subjects (Nobili et al., 2017, Sala et al., 2021). We recently demonstrated that spreading HSV-1 infection to the CNS, induced by thermal stress (TS), triggers the accumulation of AD molecular hallmarks, including amyloid beta 42, tau phosphorylation and neuroinflammation within the hippocampus, which could, in combination with dopaminergic degeneration, represent a potential mechanism for AD development (De Chiara et al., 2019, Li Puma et al., 2019). However, whether social memory and social behaviour alterations are observable in early phases of AD due to VTA-depletion or whether this can influence social preference under sickness behaviour, has not been clarified yet, as well as if these deficits manifest prior to other forms of cognitive impairments, such as spatial memory alterations.

The heaviest limitation from our study is that our results are obtained

on male adult mice and future works will be necessary to understand whether the same processes are influenced by sex and age. Given the existence of sexual dimorphism in endotoxins and pathogenic responses, it will be necessary to characterize, in detail, the response of female mice, to better generalize our findings (Yee and Prendergast, 2010). Secondarily, it will be necessary to understand whether, in the VS, different sub-regions, mediate the observed behaviour, and whether these regions may show different sensitivity to neuroinflammatory signalling. Furthermore, more nuanced analyses, such as region-specific chemogenetic control of microglial activity, will be necessary to move our correlative analysis to a more definitive causal relationship between VS-neuroinflammation and social memory. Collectively, our results demonstrate that neuroinflammation can impact social memory and that inflammatory signalling within the VS, when there is no inflammation within the hippocampus, can alter memory retrieval toward known stimuli compared to unknown stimuli. Further experiments will be necessary to clarify the precise mechanisms leading to these phenotypes and whether such alterations may be early symptoms as well as early pharmacological targets of neurodegenerative/neuropsychiatric pathologies.

CRediT authorship contribution statement

M. Rinaudo: Writing – review & editing, Writing – original draft, Project administration, Methodology, Investigation, Formal analysis, Data curation, Conceptualization. **S. Autelitano:** Writing – review & editing, Methodology, Investigation, Formal analysis. **C. D'Amelio:** Methodology, Investigation, Formal analysis. **I.Nifo Sarrapochiello:** Methodology, Investigation, Formal analysis. **G. Puliatti:** Methodology, Investigation. **G. Boni:** Methodology, Investigation. **R. Sollazzo:** Methodology, Investigation. **D.D. Li Puma:** Writing – review & editing, Supervision, Methodology. **F. Paciello:** Writing – review & editing, Supervision, Formal analysis, Data curation. **F. Natale:** Writing – review & editing, Supervision, Investigation, Formal analysis. **V. Protto:** Methodology. **G. De Chiara:** Writing – review & editing, Supervision. **R. Piacentini:** Writing – review & editing, Supervision, Conceptualization. **S. Fusco:** Writing – review & editing, Writing – original draft, Supervision, Conceptualization. **C. Grassi:** Writing – review & editing, Supervision, Conceptualization.

Funding

This work was supported by PNRR Programme "A multiscale integrated approach to the study of the nervous system in health and disease" – MNESYS Code PE00000006 to C.G.

Declaration of competing interest

The authors declare that they have no known competing financial interests or personal relationships that could have appeared to influence the work reported in this paper.

Acknowledgements

The authors would like to acknowledge the contribution of Experimental Models Research Core Facility G-STeP of Fondazione Policlinico Universitario 'A. Gemelli' IRCCS. Ministero della Salute – Ricerca Corrente 2026.

Author contribution

MR, DDLP, RP, SF and CG designed the research, drafted the manuscript and provided critical revisions; MR, SA and CD performed behavioural experiments and analysis; SA and FP performed immunofluorescence experiments and analyses; INS and FN performed molecular experiments and analyses; GDC, VP, GP, GB and SR managed the HSV-1 mouse model. All authors have reviewed and approved the final manuscript.

Appendix A. Supplementary data

Supplementary data to this article can be found online at https://doi.org/10.1016/j.bbi.2026.106879.

Data availability

Data will be made available on request.

References

Ambi A. The Copper-Gut-Brain Axis: A Triple Inflammatory Pathway Driving Neuroinflammation in Alzheimer's Disease. Aging Dis. Published online May 4, 2026. doi:10.14336/AD.2026.0375.

Bandiera B et al. Olfactory stimulation with multiple odorants prevents stress-induced cognitive and psychological alterations. *Brain Commun*. 2024;6(6):fcae390. Published 2024 Nov 5. doi:10.1093/braincomms/fcae390.

Beier, E.E., Neal, M., Alam, G., Edler, M., Wu, L.J., Richardson, J.R., 2017. Alternative microglial activation is associated with cessation of progressive dopamine neuron loss in mice systemically administered lipopolysaccharide. Neurobiol Dis. 108, 115–127. https://doi.org/10.1016/j.nbd.2017.08.009.

Ben-Shaanan, T.L., et al., 2016. Activation of the reward system boosts innate and adaptive immunity. Nat Med. 22 (8), 940–944. https://doi.org/10.1038/nm.4133.

Bilbo, S.D., Klein, S.L., DeVries, A.C., Nelson, R.J., 1999. Lipopolysaccharide facilitates partner preference behaviors in female prairie voles. Physiol Behav. 68 (1–2), 151–156. https://doi.org/10.1016/s0031-9384(99)00154-7.

Brown GC. The endotoxin hypothesis of neurodegeneration. J Neuroinflammation. 2019; 16(1):180. Published 2019 Sep 13. doi:10.1186/s12974-019-1564-7.

Chen, P., Hong, W., 2018. Neural Circuit Mechanisms of Social Behavior. Neuron. 98 (1), 16–30. https://doi.org/10.1016/j.neuron.2018.02.026.

De Chiara, G., et al., 2019. Recurrent herpes simplex virus-1 infection induces hallmarks of neurodegeneration and cognitive deficits in mice. PLoS Pathog. 15 (3), e1007617. https://doi.org/10.1371/journal.ppat.1007617. Published 2019 Mar 14.

Deleplanque, B., Vitiello, S., Le Moal, M., Neveu, P.J., 1994. Modulation of immune reactivity by unilateral striatal and mesolimbic dopaminergic lesions. Neurosci Lett. 166 (2), 216–220. https://doi.org/10.1016/0304-3940(94)90489-8.

DiSabato, D.J., Quan, N., Godbout, J.P., 2016. Neuroinflammation: the devil is in the details. J Neurochem. 139 Suppl 2(Suppl 2), 136–153. https://doi.org/10.1111/jnc.13607.

Eisenberger, N.I., Moieni, M., Inagaki, T.K., Muscatell, K.A., Irwin, M.R., 2017. In Sickness and in Health: The Co-Regulation of Inflammation and Social Behavior. Neuropsychopharmacology. 42 (1), 242–253. https://doi.org/10.1038/npp.2016.141.

Felger, J.C., et al., 2016. Inflammation is associated with decreased functional connectivity within corticostriatal reward circuitry in depression. Mol Psychiatry. 21 (10), 1358–1365. https://doi.org/10.1038/mp.2015.168.

Gorina, Y.V., et al., 2022. The Role of Neuroinflammation in Cognitive Functions and Social Interaction in Mice with Age-Dependent Neurodegeneration. Hum Physiol 48, 979–983. https://doi.org/10.1134/S0362119722080035.

Hitti, F.L., Siegelbaum, S.A., 2014. The hippocampal CA2 region is essential for social memory. Nature. 508 (7494), 88–92. https://doi.org/10.1038/nature13028.

Hunter, R.L., et al., 2009. Intrastriatal lipopolysaccharide injection induces parkinsonism in C57/B6 mice. J Neurosci Res. 87 (8), 1913–1921. https://doi.org/10.1002/jnr.22012.

Inagaki, T.K., et al., 2015. The role of the ventral striatum in inflammatory-induced approach toward support figures. Brain Behav Immun. 44, 247–252. https://doi.org/10.1016/j.bbi.2014.10.006.

Izumi, Y., et al., 2021. A Proinflammatory Stimulus Disrupts Hippocampal Plasticity and Learning via Microglial Activation and 25-Hydroxycholesterol. J Neurosci. 41 (49), 10054–10064. https://doi.org/10.1523/JNEUROSCI.1502-21.2021.

Jung H et al. Differential Regional Vulnerability of the Brain to Mild Neuroinflammation Induced by Systemic LPS Treatment in Mice. *J Inflamm Res*. 2022;15:3053-3063. Published 2022 May 23. doi:10.2147/JIR.S362006.

Kawasaki, Y., Zhang, L., Cheng, J.K., Ji, R.R., 2008. Cytokine mechanisms of central sensitization: distinct and overlapping role of interleukin-1beta, interleukin-6, and tumor necrosis factor-alpha in regulating synaptic and neuronal activity in the superficial spinal cord. J Neurosci. 28 (20), 5189–5194. https://doi.org/10.1523/JNEUROSCI.3338-07.2008.

Kopach, O., Kao, S.C., Petralia, R.S., Belan, P., Tao, Y.X., Voitenko, N., 2011. Inflammation alters trafficking of extrasynaptic AMPA receptors in tonically firing lamina II neurons of the rat spinal dorsal horn. Pain. 152 (4), 912–923. https://doi.org/10.1016/j.pain.2011.01.016.

Kopec, A.M., Smith, C.J., Bilbo, S.D., 2019. Neuro-Immune Mechanisms Regulating Social Behavior: Dopamine as Mediator? Trends Neurosci. 42 (5), 337–348. https://doi.org/10.1016/j.tins.2019.02.005.

Leroy, F., et al., 2023. The role of meat in the human diet: evolutionary aspects and nutritional value. Anim Front. 13 (2), 11–18. https://doi.org/10.1093/af/vfac093. Published 2023 Apr 15.

Li, H., Zhao, Z., Jiang, S., Wu, H., 2025. Brain circuits that regulate social behavior. Mol Psychiatry. 30 (7), 3240–3256. https://doi.org/10.1038/s41380-025-03037-6.
Li Puma, D.D., et al., 2019. Herpes Simplex Virus Type-1 Infection Impairs Adult Hippocampal Neurogenesis via Amyloid-β Protein Accumulation. Stem Cells. 37 (11), 1467–1480. https://doi.org/10.1002/stem.3072.
Li Puma DD et al. Interleukin 1β triggers synaptic and memory deficits in Herpes simplex virus type-1-infected mice by downregulating the expression of synaptic plasticity-related genes via the epigenetic MeCP2/HDAC4 complex. *Cell Mol Life Sci*. 2023;80 (6):172. Published 2023 Jun 1. doi:10.1007/s00018-023-04817-5.
Lier J, Streit WJ, Bechmann I. Beyond Activation: Characterizing Microglial Functional Phenotypes. Cells. 2021;10(9):2236. Published 2021 Aug 28. doi:10.3390/cells10092236.
Liu, M., Bing, G., 2011. Lipopolysaccharide animal models for Parkinson's disease. Parkinsons Dis. 2011, 327089. https://doi.org/10.4061/2011/327089.
Lohrenz, T., Kishida, K.T., Montague, P.R., 2016. BOLD and its connection to dopamine release in human striatum: a cross-cohort comparison. Philos Trans R Soc Lond B Biol Sci. 371 (1705), 20150352. https://doi.org/10.1098/rstb.2015.0352.
Meijer, O.C., de Lange, E.C., Breimer, D.D., de Boer, A.G., Workel, J.O., de Kloet, E.R., 1998. Penetration of dexamethasone into brain glucocorticoid targets is enhanced in mdr1A P-glycoprotein knockout mice. Endocrinology. 139 (4), 1789–1793. https://doi.org/10.1210/endo.139.4.5917.
Meira T, Leroy F, Buss EW, Oliva A, Park J, Siegelbaum SA. A hippocampal circuit linking dorsal CA2 to ventral CA1 critical for social memory dynamics. *Nat Commun*. 2018;9 (1):4163. Published 2018 Oct 9. doi:10.1038/s41467-018-06501-w.
Mercurio, D., et al., 2022. Protein Expression of the Microglial Marker Tmem119 Decreases in Association With Morphological Changes and Location in a Mouse Model of Traumatic Brain Injury. Front Cell Neurosci. 16, 820127. https://doi.org/10.3389/fncel.2022.820127. . Published 2022 Feb 10.
Moieni, M., Eisenberger, N.I., 2018. Effects of inflammation on social processes and implications for health. Ann N Y Acad Sci. 1428 (1), 5–13. https://doi.org/10.1111/nyas.13864.
Muir, J., et al., 2020. Ventral Hippocampal Afferents to Nucleus Accumbens Encode Both Latent Vulnerability and Stress-Induced Susceptibility. Biol Psychiatry. 88 (11), 843–854. https://doi.org/10.1016/j.biopsych.2020.05.021.
Murugan, M., et al., 2017. Combined Social and Spatial Coding in a Descending Projection from the Prefrontal Cortex. Cell. 171 (7), 1663–1677.e16. https://doi.org/10.1016/j.cell.2017.11.002.
Nakajima, S., et al., 2026. Anxiety induced by systemic inflammation involves microglial engulfing of nucleus accumbens inputs and diminished excitability of dopamine D1 receptor neurons. Brain Behav Immun. 131, 106154. https://doi.org/10.1016/j.bbi.2025.106154.
Natale, F., et al., 2024. Inhibition of zDHHC7-driven protein S-palmitoylation prevents cognitive deficits in an experimental model of Alzheimer's disease. Proc Natl Acad Sci U S A. 121 (49), e2402604121. https://doi.org/10.1073/pnas.2402604121.
Natale F, Spinelli M, Rinaudo M, et al. Maternal High Fat Diet Anticipates the AD-like Phenotype in 3xTg-AD Mice by Epigenetic Dysregulation of Aβ Metabolism. *Cells*. 2023;12(2):220. Published 2023 Jan 4. doi:10.3390/cells12020220.
Nobili, A., et al., 2017. Dopamine neuronal loss contributes to memory and reward dysfunction in a model of Alzheimer's disease. Nat Commun. 8, 14727. https://doi.org/10.1038/ncomms14727. . Published 2017 Apr 3.
Okuyama, T., Kitamura, T., Roy, D.S., Itohara, S., Tonegawa, S., 2016. Ventral CA1 neurons store social memory. Science. 353 (6307), 1536–1541. https://doi.org/10.1126/science.aaf7003.
Paciello F et al. Oxidative stress and inflammation cause auditory system damage via glial cell activation and dysregulated expression of gap junction proteins in an experimental model of styrene-induced oto/neurotoxicity. *J Neuroinflammation*. 2024;21(1):4. Published 2024 Jan 4. doi:10.1186/s12974-023-02996-3.
Padilla-Coreano, N., Martínez-Rivera, F.J., 2025. How dopamine guides our social world. Pharmacol Rev. 77 (5), 100085. https://doi.org/10.1016/j.pharmr.2025.100085.
Park, M.J., Park, H.S., You, M.J., Yoo, J., Kim, S.H., Kwon, M.S., 2019. Dexamethasone Induces a Specific Form of Ramified Dysfunctional Microglia. Mol Neurobiol. 56 (2), 1421–1436. https://doi.org/10.1007/s12035-018-1156-z.
Phillips, M.L., Robinson, H.A., Pozzo-Miller, L., 2019. Ventral hippocampal projections to the medial prefrontal cortex regulate social memory. Elife. 8, e44182. https://doi.org/10.7554/eLife.44182. . Published 2019 May 21.
Protto, V., et al., 2024. HSV-1 infection induces phosphorylated tau propagation among neurons via extracellular vesicles. mBio. 15 (10), e0152224. https://doi.org/10.1128/mbio.01522-24.
Rinaudo M et al. Hippocampal Estrogen Signaling Mediates Sex Differences in Retroactive Interference. *Biomedicines*. 2022;10(6):1387. Published 2022 Jun 11. doi:10.3390/biomedicines10061387.
Rogers, J.F., Vandendoren, M., Prather, J.F., Landen, J.G., Bedford, N.L., Nelson, A.C., 2024. Neural cell-types and circuits linking thermoregulation and social behavior. Neurosci Biobehav Rev. 161, 105667. https://doi.org/10.1016/j.neubiorev.2024.105667.
Ruan, C., Elyaman, W., 2022. A New Understanding of TMEM119 as a Marker of Microglia. Frontiers in cellular neuroscience 16, 902372. https://doi.org/10.3389/fncel.2022.902372.
Sala A et al. In vivo human molecular neuroimaging of dopaminergic vulnerability along the Alzheimer's disease phases. Alzheimers Res Ther. 2021;13(1):187. Published 2021 Nov 12. doi:10.1186/s13195-021-00925-1.
Sheppard, O., Coleman, M.P., Durrant, C.S., 2019. Lipopolysaccharide-induced neuroinflammation induces presynaptic disruption through a direct action on brain tissue involving microglia-derived interleukin 1 beta. J Neuroinflammation. 16(1): 106. https://doi.org/10.1186/s12974-019-1490-8. Published 2019 May 18.
Sholl DA. The measurable parameters of the cerebral cortex and their significance in its organization. *Prog Neurobiol (1956)*. 1956;(2):324-333.
Smith, J.A., Das, A., Ray, S.K., Banik, N.L., 2012. Role of pro-inflammatory cytokines released from microglia in neurodegenerative diseases. Brain Res Bull. 87 (1), 10–20. https://doi.org/10.1016/j.brainresbull.2011.10.004.
Soares-Cunha, C., et al., 2020. Nucleus accumbens medium spiny neurons subtypes signal both reward and aversion. Mol Psychiatry. 25 (12), 3241–3255. https://doi.org/10.1038/s41380-019-0484-3.
Son JY, Kwack WG, Chung EK, Shin S, Choi YJ. Effects of Early Initiation of High-Dose Dexamethasone Therapy on Pro-Inflammatory Cytokines and Mortality in LPS-Challenged Mice. *Healthcare (Basel)*. 2022;10(7):1247. Published 2022 Jul 4. doi:10.3390/healthcare10071247.
Troubat, R., Barone, P., Leman, S., et al., 2021. Neuroinflammation and depression: A review. Eur J Neurosci. 53 (1), 151–171. https://doi.org/10.1111/ejn.14720.
Vazquez S, Gold J, Spirollari E, Akmal S, Hanft SJ. The story of dexamethasone and how it became one of the most widely used drugs in neurosurgery. J Neurosurg. 2023;140 (4):1191-1197. Published 2023 Nov 24. doi:10.3171/2023.9.JNS231099.
Willette, A.A., Lubach, G.R., Coe, C.L., 2007. Environmental context differentially affects behavioral, leukocyte, cortisol, and interleukin-6 responses to low doses of endotoxin in the rhesus monkey. Brain Behav Immun. 21 (6), 807–815. https://doi.org/10.1016/j.bbi.2007.01.007.
Xu S et al. Neural Circuits for Social Interactions: From Microcircuits to Input-Output Circuits. *Front Neural Circuits*. 2021;15:768294. Published 2021 Oct 29. doi:10.3389/fncir.2021.768294.
Yamamoto, M., et al., 2025. Lipopolysaccharide-Induced Inflammatory Responses Increased Dyadic Social Interaction In Male But Not Female Mice. Int J Neuropsychopharmacol. 28 (Suppl 1), i330–i331. https://doi.org/10.1093/ijnp/pyae059.590. Published 2025 Feb 12.
Yee, J.R., Prendergast, B.J., 2010. Sex-specific social regulation of inflammatory responses and sickness behaviors. Brain Behav Immun. 24 (6), 942–951. https://doi.org/10.1016/j.bbi.2010.03.006.
Yong SJ et al. The Hippocampal Vulnerability to Herpes Simplex Virus Type I Infection: Relevance to Alzheimer's Disease and Memory Impairment. Front Cell Neurosci. 2021;15:695738. Published 2021 Aug 13. doi:10.3389/fncel.2021.695738.
Zhang J et al. LPS activates neuroinflammatory pathways to induce depression in Parkinson's disease-like condition. *Front Pharmacol*. 2022;13:961817. Published 2022 Oct 6. doi:10.3389/fphar.2022.961817.
Zhang W, Xiao D, Mao Q, Xia H. Role of neuroinflammation in neurodegeneration development. *Signal Transduct Target Ther*. 2023;8(1):267. Published 2023 Jul 12. doi:10.1038/s41392-023-01486-5.
Zorab, J.M., et al., 2025. Serotonin and neurotensin inputs in the vCA1 dictate opposing social valence. Nature. 642 (8066), 154–164. https://doi.org/10.1038/s41586-025-08809-2.